The Effect of Ship Transport on Fast Ice Stability: Lac St. Pierre, Quebec.

Edward J. Stander[1], Donald Carter[2], Brian Morse[3]

[1]State University of New York at Cobleskill, Cobleskill, NY, USA 12043.
Standeej@Cobleskill.Edu
[2]Carter Associates, 1281 Rue Bishop, Sainte-Foy, QC, Canada. G1W 3E4.
Carter@Mediom.qc.ca
[3]Previously with the Canadian Coast Guard during the time of the field study, now with Dept. Genie Civil, Université Laval, Sainte-Foy, QC, Canada. G1K 7P4.
Brian.Morse@gci.ulaval.ca

Abstract

Lac St. Pierre is a wide segment of the St. Lawrence River located downriver of Montreal, and bounded by the towns of Sorel to the west and Trois-Rivières to the east. Ship transport occurs throughout the winter season, and has, in the past, led to the catastrophic break-up of the ice sheet close to shore, and the spalling of large ice floes into the navigation channel. These loose flows are undesirable elements of winter navigation as they can push ships onto shoal areas outside of the channel and initiate ice jams at the LaViolette Bridge located immediately downriver of the lake.

This paper describes the results of a field program carried out for the Canadian Coast Guard in 1995 that was designed to pinpoint the causes of ice breakup along the border of the navigation channel. Stress and ice displacement gages were deployed at several distances from the channel, and continuous measurement made as a variety of transport ships crossed the study area. Of the forty vessels studied, only two seriously damaged the ice border, and these turned out to be unremarkable in size and gross tonnage. Subsequent analysis of the acquired data set showed that damage was caused by ice flexure during drawdown, and suggests that ship draft, length, and speed together controlled fracture development at the ice front.

1. **Introduction**

The stability of the fast ice sheet in Lac St Pierre is important for a number of reasons. First, the sheet supports an active ice fishing community which relies on the stability of the ice cover for its operations. Secondly, ice floes spalling into the navigation channel can severely damage passing ships and can initiate ice jams particularly at the fixed structures located downstream (such as the LaViolette bridge at Trois-Rivières).

The presence of the new ice boom at Yamachiche has greatly improved the stability of the fast ice cover along the north side of the lake. However, degradation of the cover still occurs as a result of ship transport through the St. Lawrence navigation channel. Waves generated by passing ships commonly break floes off the leading edge of the ice sheet, and have been known to produce large open leads in the vicinity of the shoreline.

The present study was undertaken to improve our understanding of the manner in which transport ships interact with the ice sheet, and to offer guidelines which might assure the continued stability of the cover without excessively penalizing carriers who use the channel during the winter months. The findings of this study have been used by the Canadian Coast Guard to determine and issue recommended maximum commercial vessel speeds in the St.Lawrence River between Trois-Rivières and Montréal, particularly during the ice formation period. Since implementation, the cover has proved to be much more stable.

2. **The Field Program**

The Lac St. Pierre ice cover underwent three stages of development over the winter of 1995. The first fast ice sheet formed overnight on December 12, and melted shortly after December 20. The second sheet developed early in January, 1995, but suffered periods of melting and rotation prior to final stabilization in mid January. This greatly curtailed the length of the field program, as the ice was not considered safe to walk on prior to the end of January (Carter, Stander and Hodgson, 1995).

Deployment of equipment began on February 3, following a week of calibration and preparation at Université Laval in Quebec City. Ice thickness within the main ice sheet at that time varied from 30 - 40 cm, but decreased in the ice sheet immediately adjacent to the navigation channel. It was thus decided to place the stress and displacement gages at the boundary between the *in situ* ice sheet and the rubble apron, approximately 700 m from the ice edge. The ice sheet located south of this boundary was not considered competent enough to support human activity.

Fortunately, sub-seasonal temperatures during the week following installation led to the rapid consolidation of the ice apron, and allowed us to move several of the gages to new sites closer to the ice edge on February 14. Two of these sites (sites F and G - see figure 1), were located on a previously unfrozen region, now consisting of 20 cm of perfectly clear S1 ice. The third site (Site H), was located in the rubble apron, 85 m from the ice edge. This latter site was fully operational until Feb. 20, when it was evacuated due to the spalling of adjacent ice into the channel.

Removal of the remaining gages took place on Saturday, Feb. 25, immediately prior to the

arrival of the hydrofoil responsible for removal of the ice cover.

3. **Methodology**

Two principal gage types were used during this study. In-plane (biaxial) ice stresses were measured with the aid of four three-wire GEOKON stress transducers fabricated by Geokon of Lebanon, New Hampshire (Cox and Johnson, 1983). These gages consist of a thick walled hollow cylinder, 5.7 cm in diameter and 7.5 cm in length, which supports two vibrating wire strain transducers oriented 90 degrees to the long axis of the cylinder and 90 degrees to one another (figure 2). Two of these gages were placed next to one another to allow definition of the stress axes in the plane of the ice sheet. Compressive stresses as small as 10 kPa applied in the plane of the wires produced a change in the resonant frequency of all wires, and was resolvable by the data logger.

Gages at three sites were placed so that their centers lay at a nominal depth of 3 cm, while gages at site C were placed at a nominal depth of 28 cm.

Ice vertical displacement was measured at three sites using ENDECO long wire displacement transducers (figure 3). ENDECO transducers are essentially RVDTs (rotational variable differential transformers) attached to a stainless steel wire by way of a spring system. In operation, the transducer was suspended above a hole in the ice, and attached to the lake bottom by way of a weighted wire. A decrease in ice level with respect to the lake bottom produced a concomitant decrease in wire length and output voltage.

The steel wire system worked well at all sites except position H. Here, the passage of large ships produced a sudden and drastic change in wire length. Instantaneous and repeatable variations of 20-40 cm were commonly measured. These variations disappeared when the thin wire was replaced by a 3 inch diameter ABS tube hammered into the lake bottom.

Measurements were collected by two Campbell Scientific CR-10 data loggers located on site. One CR-10 was branched at Site C, while the second was located on the frozen lake at site G. Measurements were collected at two second intervals: faster measurement times led to degradation of the vibrating wire signal. Synchronization of data sets was assured by simultaneously stopping both loggers at the end of each day.

Apart from the above measurements, ice temperature was collected once a day from two platinum resistance thermometers (RTD) located at site C, while the position of each site was determined twice during the field season by DGPS. The temperature measurements were required to correct stress data for thermal effects, while the DGPS data was used to correct the timing of stress and displacement data for non-perpendicularity with respect to our reference line.

The line of reference used during this study was oriented perpendicular to the navigation channel, and passed through site C. All events (ship passages, stress/displacement events, etc.) were referenced to this line. This allowed us to define the effect of ship position on ice deformation in space as well as time during subsequent analyses.

4. **Results**

4.1. **Macroscopic observations**

The main ice sheet (that part of the sheet exclusive of the rubble apron) consisted of flat, pristine fast ice, 30-40 cm in thickness. Snow cover was minimal (1-10 cm) throughout most of the season, as most snow was blown off the sheet as soon as it fell.

The absence of snow cover, and the effects of strong sunlight led to the formation of large tension cracks during the night of February 12. These cracks segmented the rubble apron into numerous elongate blocks, and were more or less active throughout the day. Maximum ice thickness in the healed fractures was on the order of 2-3 cm.

Interestingly enough, no measured lateral displacement/refracturing was observed across any of these fractures during the day, despite the passage of two large container ships (the CANMAR Valiant and the Chippewa). Complete healing of the fractures occurred overnight.

The second observed macroscopic event occurred on February 18, shortly after the passage of the CCAL Thorscape. This ship produced audible, high frequency cracking noises in the ice sheet similar to the firing of a rifle, which could be heard long before the ships' arrival at the measurement site. Similar sounds were reported from the nearshore environment by one of the authors (D.C.).

While no evident displacement of the ice cover was noted immediately after the passage of the Thorscape, spalling of the ice sheet soon followed, with the result that 50 m of the rubble apron was lost during the day, and 15 m more was lost overnight. Further regression continued during the following days, culminating with the evacuation of site H on February 20.

Fractures associated with these spalling events were readily observed in the rubble apron, and were generally parallel to the ice edge. Spacing between cracks was on the order of 8-9 meters near the edge, and increased shorewards. The cracks themselves widened upwards and were rarely more than 2-3 mm in width.

Shoreline flooding was also observed at several locations during the following days, and may have been related to the passage of the Thorscape. No unusual deformational features were noted in the main ice sheet.

4.2. **Ice displacement**

Ice displacement and stress measurements were collected from 40 ship events. Thirteen of these events occurred prior to Feb. 14, and consist of records collected far from the ice edge (> 600 m). An attempt to collect data nearer the ice edge led to the occupation of sites D and E on Feb. 10 and 11, respectively.

Events subsequent to Feb. 14 were collected from sites F and G (or H). Site G replaced site H late in the season (Feb. 20) when the latter became untenable.

The typical ice displacement event was readily divisible into four phases (figure 4). During phase I, the approaching ship forced the ice sheet to gradually rise 1-3 cm above its equilibrium level. In the majority of cases, this rise was immediately preceded by a slight depression of ice level, although this was not seen at relative ship velocities higher than 8 knots.

In phase II, the ice sheet underwent a rapid depression below its equilibrium level. The amount of depression appears to have depended on two parameters: the ship's velocity (relative to water velocity), and the displacement of water associated with the ship's passage (ie. its drawdown). Maximum depression for the present study was obtained from the CANMAR Fortune, a container ship which displaced the ice sheet 20 cm below its equilibrium level.

Phase III was present in most, but not all, of the displacement events, and was rarely observed at distances greater than 600 m from the ice edge. This phase was marked by a slight rise and depression, or rise and leveling off of the displacement curve, at values slightly below equilibrium. It was usually followed by a slight rise above equilibrium level during phase IV.

Apart from arching the ice sheet slightly above its original level, Phase IV was also characterized by small, rapid 'chattering' events, in which ice level fluctuated 3-5 mm in the span of 2-4 seconds. These events were relatively uncommon, as they were only observed in 4-5 records: yet once begun, the small scale oscillations continued long after the phase had concluded. Their importance will be considered further in section 5 below.

4.3. **Stress measurements**

Despite major fluctuations in ice level with the passage of a given vessel, changes in ice stress during a given ship event were generally modest. Stress events at distances greater than 600 m from the ice front were negligible, while events closer to the channel rarely topped 100 kPa.

The most common stress event was a general lowering of compressive stresses during the passage of the phase II displacement wave. This lowering of stress state, which in some cases was greater than 100 kPa, was best observed near the ice edge. There, both maximum and minimum stress were equally affected, and remained affected for hours after the event. Further into the ice sheet (> 150 m from the ice edge), the stress event was more deviatoric in character, with an increase in maximum stress being offset by a decrease in minimum stress.

The magnitude of stress associated with a given ship event was proportional to the depth of ice depression suffered during the phase II displacement event. Ice displacements smaller than 5 cm were effectively ignored by the cover near the ice edge and produced only moderate deviatoric effects further shoreward. An exception to this rule were the 'chattering' events which were apparently insensitive to ice displacement. These events produced rapid fluctuations in stress on the order of 100-200 kPa, which, in at least one case, persisted for more than an hour after the event. Their description, and effect on the ice sheet, will be detailed further in the next section.

5. **Case Histories**

In this section, we describe the effects of the four strongest events measured during our investigation. Event 1 was produced by the CANMAR Europe, the largest, and heaviest ship encountered during the study period. Event 2 was the product of the CANMAR Fortune, a container ship whose static draft was only slightly smaller than the Europe, and which exhibited the greatest ice depression effect measured. Event 3 involved the Sachsen, a heavy container ship which exhibited the highest relative velocity of any ship measured, while event 4 was produced by the CCAL Thorscape, the ship which we believe was responsible for much of the damage suffered by the ice front during our investigation.

5.1. **The CANMAR Europe**

The CANMAR Europe is a large container ship having a gross tonnage in excess of 30000 tonnes, an overall length of 231 m and a static draft of 10.1 m. When encountered, the Europe was moving at a relative velocity of 7.7 knots (10.8 knots absolute velocity) downstream.

5.1.1. **Ice displacement**

Figure 5a shows the effect of the CANMAR Europe on ice displacement. In this diagram, the spatial position of the Europe with respect to ice displacement is maintained, while the vertical scale of ice displacement is greatly exaggerated (1:1000) to facilitate observation of their salient features. Movement of the ship was from left to right .

The displacement waves, measured 95, 180, and 545 m from the ice edge, were essentially identical. All three waves displayed the four phases of displacement discussed in section 4.2. above, although the wave measured closest to the shore have been attenuated somewhat by distance.

The first observation to be had from this diagram is one of scale. The presence of the rapidly approaching Europe was felt by the ice sheet nearly 1.5 km ahead of the vessel. Closer to the vessel (< 600 m), the ice began its slow rise above equilibrium, followed by a rapid descent during phase II. The degree of depression measured during this latter phase was 8 cm near the ice edge, and 6 cm further shoreward. Phase III followed closely behind phase II, and consisted of a small rise and descent below equilibrium. This was followed by a muted phase IV, which produced a rise approximately equal to that of phase I (1.5 cm). Taken together, the four phases affected more than three linear kilometers of ice front at any given moment.

The velocity of wave propagation into the ice sheet was on the order of 8.4 m/sec, giving a wave front oriented 56 degrees to the ice edge. If we extrapolate this front into the channel, we find that the trough of the phase II depression neatly coincides with the bow of the Europe.

5.1.2. **Ice stress**

Figure 5b provides stress data from the two sites in operation during the passage of the Europe (sites C and G). Site H was non-operational at the time. As with figure 5a, spatial relationships were maintained in the preparation of this figure.

In-ice stresses associated with the passage of the Europe were small and localized, the only observable evidence of the ship's presence being a 100 kPa rise in stress coinciding with the passage of the phase II ice depression. If we consider the level of stress occurring between any two adjacent readings (i.e. the instantaneous stress), evidence for the passage of the vessel disappears completely. This in turn suggests that the ice sheet accommodated the passing of the Europe without suffering fracture or permanent plastic deformation.

5.2. **The CANMAR Fortune**

The CANMAR Fortune is a container ship, similar in profile to the CANMAR Europe, but slightly smaller (185 m in length compared to 215 m for the Europe). While its gross tonnage was also smaller than the Europe (20000 tonnes), its static draft was somewhat greater (10.65 m). When encountered, the Fortune was moving at a relative velocity of 7.7 knots (10.8 knots absolute velocity) downstream.

5.2.1. **Ice displacement**

The general form of the ice displacement curve was similar to that of the Europe (compare figures 5a and 6a). Phase I consisted of a muted rise and trough which culminated in a 3 cm arch 600 m ahead of the vessel. Although the total length of the phase was similar to that of the Europe (1.5 km), the various components of the phase were generally less obvious.

The ice depression associated with phase II was very well developed, and bottomed out 20 cm below the equilibrium level of the ice sheet (9 cm at site C). This was the single greatest depression measured during this study. In contrast, phase III was much shorter, and consisted mainly of a level plateau, 400 m in length, wherein the ice sheet lay 1-2 cm below its equilibrium level.

Phase IV was also smaller than observed in the Europe. The rise in ice level associated with phase IV began approximately 800-1000 m behind the passing ship, and ended 200 m further upstream. The maximum observed rise was on the order of 2 cm.

The displacement wave front produced by the Fortune lay 50 degrees from the trend of the navigation channel, and once again could be extrapolated to cross the bow of the passing vessel.

5.2.2. **Ice stress**

Unlike the Europe, the passage of the CANMAR Fortune produced a major disturbance in the state of stress near the ice front (fig. 6b). At site H, located 80 m from the ice edge, maximum and minimum stresses decreased simultaneously and nearly instantaneously by 100 kPa, while deeper in the ice sheet (site G), maximum stress dropped more than 200 kPa before regaining half of this loss shortly thereafter. In both cases, the sharp decrease in stress coincided with the passage of the phase II trough.

While maximum and minimum stress values displayed the effects of ice deflection, instantaneous stress values were only mildly affected by the displacement wave. Maximum

variations were on the order of 50 kPa, once again suggesting that short term events, such as fracture development, were rare.

5.3. **The Sachsen**

The Sachsen is a container ship, much like the CANMAR Fortune and Europe. Its gross tonnage is approximately 18000 T, its overall length is 174 m and its static draft was measured at 9.8 m. When encountered, the Sachsen was moving at a relative velocity of 14.3 knots (11.2 knots absolute velocity) upstream.

5.3.1: **Ice displacement**

Figure 7a provides a spatial representation of ice displacement with respect to the passing vessel. The three plotted curves, collected from sites H, G, and C, respectively, differed in several significant ways from the displacement curves produced by the Fortune and Europe.

First of all, phase I consisted of a single elongate rise, 1500 m in length, which culminated in a 3 cm high ice arch. The smaller parasitic waves present in the records of the Europe and Fortune were not observed in this record.

Secondly, phase III was more or less absent from the record. Instead, the phase II depression opened directly onto phase IV. Phase II was similar to that observed for the CANMARs, with maximum values of 16.45 cm being measured near the ice edge, and 5.1 cm being measured at site C. Phase IV was different in that small rapid fluctuations in ice level ('chattering') were pervasive throughout the entire phase. The frequency of chattering was on the order of the sampling rate (1/2 Hz) and was quite long lived: in the case of the Sachsen, ice chattering was observed in the record 30 minutes after the ship had passed.

Typical amplitudes for ice chattering were on the order of 2-4 mm, although discrete chattering events varied in amplitude over time. This variability, however, may have been the result of the sampling rate, which was probably not fast enough to avoid aliasing of the data set.

A final difference between the Sachsen and the majority of ship events was the velocity of propagation of the displacement wave shorewards. The average velocity measured for the Sachsen was twice that of the two CANMARs (> 16 m/sec), producing a wave front oriented 71 degrees to the navigation channel (figure 7a). Still, given even this extreme propagation velocity, the extrapolated wave front neatly followed the bow of the passing vessel.

5.3.2. **Ice stress**

In general, stress effects associated with the passing of the Sachsen were quite small (figure 7b). The stress drop noted during the Fortune event was present, as was the deviatoric rise in maximum stress noted during the Europe event: yet the maximum stress difference measured with the passing of the Sachsen was on the order of 60 kPa.

The most distinctive feature of the Sachsen record was the high frequency component of stress associated with chattering events. Chattering of the ice sheet produced cyclical stress variations

on the order of 50 kPa, which were well developed far into the ice sheet. Their contribution to the total stress picture is most evident in the instantaneous stress record, wherein they can be seen to effectively disrupt the previously quiescent ice. Their development as a result of flexure at the bottom of the phase II trough is also evident from this figure.

While no evident cracking was observed following the passage of the Sachsen, the loss of 40 m of ice edge during the evening following its passage may indicate that fracturing of the ice sheet did indeed occur.

5.4. **The CCAL Thorscape**

The Thorscape is a cargo ship having a profile quite different from the three preceding vessels. Indeed, its sharply pointed bow set it off from all other ships encountered during this study. The Thorscape was also the first vessel to unquestionably damage the ice edge.

The Thorscape is a small ship when compared to the Sachsen, Fortune, and Europe. Its gross tonnage is half that of the Sachsen (9732 tonnes) and its static draft was the smallest of the four (9.3 m), as was its overall length (165 m). When encountered, the Thorscape was moving at a relative velocity of 12.5 knots (8.7 knots absolute velocity) upstream.

One feature worth noting: the Thorscape, and its sister ship, the Thor #1, passed by the Yamachiche ice boom three times during the course of this study, yet it was only on the upstream voyage that the ice sheet suffered extensive damage from its passage.

5.4.1. **Ice displacement**

The ice displacement record of the Thorscape contained elements of both the Sachsen and the two CANMARs (figure 8a). Phase I was essentially identical to the Sachsen, and consisted of a 1000 m long ramp culminating in a 4 cm high ice ridge. Phase II was also similar, with the maximum ice depression attaining a value of 15 cm near the ice edge (site H), and 14 cm at site F.

Phase III was well developed in the Thorscape record, although its lateral extent was much less than that of the Fortune or Europe. Both upwarping and downwarping of the ice sheet were evident, with total throw being on the order of 2 cm.

Behind the phase III warping, a slight rise (<3 cm) marked the start of phase IV which, once again, was of much smaller lateral extent than the other three ships. Taken together, the total length of the ice displacement event was on the order of 1800 m, provided that one ignores the presence of ice chattering.

Ice chattering was prevalent during phases II, III and IV, and was observed, albeit to a lesser extent, more than an hour later in the records of subsequent ship events. While the frequency of discrete chattering events was identical to that noted with the Sachsen, the maximum amplitude of each event was greater, despite the fact that the measurement site was located 40 m further into the ice sheet during the Thorscape event.

5.4.2. **Ice Stress**

The ice stress record of the Thorscape was essentially an exaggerated copy of the Sachsen (fig 7b and 8b; also see figure 9.). The passage of the phase II trough produced a decrease in maximum and minimum stress, as well as a sharp 100 kPa stress peak immediately beneath the depression. Instantaneous stress variations were also similar to those measured during the Sachsen event, with instantaneous stress variations of 100-150 kPa commonly occurring behind the phase II trough.

6. **Discussion**

The results presented above support the belief that ships passing through the Lac St Pierre navigation channel can structurally damage the adjacent fast ice sheet. They also support the empirical observation that not all ships cause damage, and that the same ship on different occasions may produce entirely different effects on the ice sheet. In this section, we present a discussion of the parameters we feel are responsible for ice damage, as well as preliminary suggestions for assessing the relative impact of future ship events.

6.1. **Ice failure**

Indications from the records of the CCAL Thorscape and Sachsen suggest that ice failure was associated with the passage of the phase II displacement event. In particular, it appears that the trough of the phase II depression acted as the loci for rupture. While it is not certain what importance the subsequent chattering events had on deformation, it is likely that these further aggravated the situation by causing the ice sheet to fail through fatigue.

The most important parameter to consider in defining the impact of a passing ice wave on ice sheet integrity seems to have been its radius of curvature. Ice is relatively weak in flexure, and typically fails in tension during bending tests. Several studies have shown that the maximum supportable flexure deformation of a thin ice sheet is approximately 30 % of its thickness (Gold, 1971). Thus, it is relatively safe to argue that the Lac St Pierre ice sheet will only support a certain limiting flexure before failure occurs.

In the case of the present study, only one (or possibly two) ships were observed to damage the rubble apron. Significantly enough, these two ships also displayed the smallest radius of trough curvature of all vessels measured. Figure 10 provides an enlargement of the phase II troughs for the four ship events discussed above. As can be seen, the Thorscape event displayed the smallest radius of trough curvature, followed by the Sachsen, the Fortune, and the Europe.

If a limit for ice curvature does indeed exist, it certainly falls between that exhibited by the Sachsen and the two CANMARs.

6.2. **Development of the ice trough**

The question must now focus on what parameters define the radius of curvature of the phase II

trough. The position of the trough with respect to the passing ship leaves little doubt that it marks the passage of the ships draw-down wave beneath the ice cover. Draw-down occurs when the waters of the navigation channel are forced to flow about the ships hull. This major obstacle to flow forces the current velocity on either side of the hull to increase, leading to the lowering of water level in the immediate vicinity of the ship.

Provided that the phase II trough does indeed mark the position of the ships draw-down wave, we can hypothesize that the following external parameters will directly influence the radius of trough curvature:

A) Ship velocity: the magnitude of the drawdown wave is strongly affected by ship velocity. The greater the velocity, the greater the energy associated with the passage of the vessel, and the deeper the draw-down waves.

B) Ice thickness: The thicker the ice sheet, the greater the tensional and compressive stresses developed along its free surfaces.

C) Ice temperature: The warmer the ice sheet, the more pliable it becomes

D) The form of the draw-down and draw-up waves: Any asymmetry present in the two waves can only aid in producing an asymmetric flexure in the overlying ice sheet. This in turn will further steepen the ice descent into the phase II trough.

Thus ice conditions, wave characteristics, and velocity will together influence the depth of the trough, and the radius of curvature apparent at its base.

6.3 Comparison of observed stresses to analytical solutions.

While numerous authors have considered the nature of wave/ice interactions (see, for example, papers by Daly, Squire, Steffler and Hicks and Xia and Shen), we will limit our discussion here to the theory proposed by Beltaos (2004). His analysis is based on the specific boundary conditions of a wave entering an ice sheet modeled as an elastic foundation (with no inertial terms considered).

According to figure 10 of the Beltaos paper, the half wave length of the drawdown trough corresponds to a little more than the ship's length; i.e., $L/2 \sim 250$ m. Then the wave number $k = 2p/L = 0.013$ m^{-1}. Also, let us suppose that the average ice thickness is h = 0.4 m and that Young's modulus E = 6GPa. Then the characteristic wave length ($l \sim 15\, h^{0.75}$) of the ice is $l =$ 7.6 m and $kl = 0.10$.

According to Beltaos, for $kl < 0.34$, the dimensionless bending stress is $S_p \sim 0.16kl$ corresponding to $S_p \sim 0.016$. Since the wave amplitude is $w_o = 0.19$ m, and since S_p corresponds to $l^2 s/(hw_oE)$, the theoretical maximum stress in the ice is s = 130 kPa. This corresponds very well to the observed increases in compressive stresses of 80 to 100 kPa recorded near the ice edge (figures 6 to 9 below), which, extrapolated to top of ice conditions (multiply by 20/17) gives 90 to 120 kPa.

According to figure 9 below, prior to the arrival of the Thorscape, the main principal compressive stress in the ice near the edge was approximately 270 kPa. As the bow wave reached the gage, it fell by 50 kPa to 220 kPa. Then as the trough wave passed, it jumped up to 360 kPa at which time there was an important failure event in the ice sheet. Subsequently, the main principal compressive stress stabilized at about 210 kPa. For technical reasons, we were unable to measure tensile stresses in the ice at this site near the ice edge. However, if the neutral axis is near the center of the ice sheet, we can assume that principal tensile stresses will be similar and opposite to principal compressive stresses. Therefore, the maximum principal tensile stress would be on the order of -360(20/17) = -420kPa. This is close to the accepted value of maximum tensile strength for failure in bending (-600kPa). The discrepancy may be due to the fact that the recorded stresses were measured at site "H" (located 85 m from the ice edge) whereas ice spalling occured at 65 m from the edge (where it is assumed that the maximum stress occured). If the stress in the ice sheet follows the example for kl = 0.25 (Beltaos, figure 4c), then a -420 kPa stess at 85 m would correspond to about a -630 kPa stess at 65 m.

Beltaos predicts (his figure 6) that, for kl = 0.1, the crack will at e ($=x/(2^{0.5}l)$) =14. Therefore, the predicted location of spalling will be at x = 120 m. Although the prediction is of the right order of magnitude, it seems to be off by a factor of two.

6.4 The chattering effect

Figure 9 below indicates that the minor principal compressive stress fell from 50 kPa prior to the ship arrival to a mean value of about 0 kPa after the ice cracked. This is consistent with a the fact that the minor principal stress must be near zero when the gage is near a free surface (as is the case when the ice ruptures).

Figure 9 below also shows that there is a high frequency stress pattern in the ice sheet after the fracture event. According to figure 8b, the period of the wavelength is about 28 m corresponding to kl = 1.7. We do not know the source of these waves however there is a good reason to believe that they are produced by the ship passage: Depending on the Froude number of the ship, it could generate four Kelvin waves along its body (44 m apart). If the angle that the waves made with respect to the ship is a reasonable 32 degrees, then their wave length would be 44 tan(32°) = 28 m. In any case, according to Beltaos (his figure 5), wave lengths $0.8 < kl < 2$ are the ones that have the potential to do the most damage. For kl = 1.7, S_p is 0.23 or 0.17 depending respectively on if the wave is entering the ice or if it has already entered.

Consider a Kelvin wave having a typical amplitude of 0.25 m near the ship that attenuates to $w_o \sim$ 0.10 m by the time it reaches the ice. Since S_p corresponds to to $l^2 s/(hw_oE)$, the theoretical maximum stress caused by the wave entering the ice sheet would be $s \sim$ -950 kPa. In almost all cases, this stress would be sufficient to fissure the ice near the edge. As the ice fissures, the wave is rapidly dampened. And there is therefore a residual pressure wave that enters the ice and travels through it but is not of sufficient amplitude to cause further failure. This could be the source of the observed chattering.

According to our measurements, the chattering has an amplitude of about w_o = 0.015 m. This corresponds to a stress fluctuation of 140 kPa perpendicular to the ice sheet and 100 kPa parallel to the ice sheet for S_p 0.23 or 0.17 respectively. These estimates agree fairly well with the observed values of 70(20/17)=80 kPa and 50(20/17)=60 kPa (figure 9 below) respectively.

When these short Kelvin waves cause failure, Beltaos predicts (his figure 6) that the crack will form at e ($=x/(2^{0.5}l)$) =1.6 corresponding to x = 17 m.

6.5. **Guidelines for ship transport within the navigation channel in winter**

Several factors must be considered in defining a maximum speed for ship transport in winter. First and foremost is the state of the ice sheet adjoining the navigation channel. Ice thickness, temperature, and structure will all control the limiting radius of curvature in the phase II trough. Indeed the balance may turn out to be quite delicate. For example, thin ice is more pliable than thick ice and may therefore be expected to sustain tighter radii of curvature without fracture. Yet, on the other hand, thicker ice sheets will develop greater surface stresses at a given radius of curvature than thin ice, and will therefore require less bending to rupture. In general, however, the thicker the ice sheet, the more readily the ice will rupture at a given velocity.

Ship velocity relative to current velocity is also important, and is a more accurate measure of the energy of ship generated waves than absolute ship velocity. Thus, all things being equal, vessels travelling upstream should have a lower absolute velocity limit than vessels moving downstream. In our study, vessels moving downstream greatly outnumbered those moving upstream, yet it was only the latter group that inflicted any sustained damage to the ice sheet.

Finally, ship design should be considered in projecting safe velocity limits. Some ships, such as the CANMARs are generally innocuous when passing through the navigation channel, while other ship designs, such as that used for the Thorscape, require lower velocity limits as their waves appear to be of much higher energy than the container ships.

7. Conclusions

Ever since Daly predicted the passage of acoustic waves through ice sheets in 1993, we have tried to observe their effects (e.g., Beltaos and Rowsell, 2001). This study on ship traffic beside a fast ice sheet would seem to provide an example how the ice sheet reacts to two specific cases of short amplitude waves. The first has a wave length of about 500 m and amplitude of 0.19 m. According to observations, the maximum induced stresses are in the order of 120 kPa and agrees within 20% with the theory proposed by Beltaos (2004) although the predicted location of the maximum stress (120 m from the edge) seems to overestimate the observed penetration (65 m) by a factor of two.

The second type of observed waves appear to originate from the Kelvin waves formed about the vessel. They are typically 28m in length and have an initial amplitude of 0.1 m. According to

Beltaos, these wave lengths are prime candidates to cause damage. At the ice edge the increase in stress about 950 kPa and could cause spalling in the order of 17 m. Although we did not observe this effect during this study, we have observed the phenomenon elsewhere. What we did observe was chattering consisting of wave lengths of approximately 28 m having amplitudes of 0.015m resonating through the sheet for many minutes once the ship had passed. The theoretical increase in stress resulting from these waves would lie between 100 and 140 kPa (depending on their orientation with respect to the ice edge). These values roughly agree with our extrapolated observed stresses of 80 and 60 kPa. We believe that the Kelvin wave amplitudes that travel through the ice sheet are limited to those values that will not fracture the ice because the initial higher amplitudes do fracture the ice near the edge and only the residual wave is allowed to penetrate into the ice.

In this analysis, we assumed that there was no superposition of the Kelvin waves on top of the drawdown wave because we believe that the drawdown arrives before the Kelvin waves. However, if the waves in phase III represent a reflection of the drawdown waves from the lake boundaries, there may be superposing of the two wave types during that time that may potentially lead to further ice fissuring.

7. **Recommendations for further work**

This study has defined some of the possible parameters responsible for ice failure, and has laid a foundation for a theoretical study on ice sheet flexure in a kinematic environment. Our first recommendation, then, is a theoretical study to support or refute the hypotheses presented in the above discussion. This model may then be applied to the problem of ice flexure in the phase II trough. What are the flexural limits of an ice sheet deformed in such an environment, and what wave energy is required to produce a stable trough geometry having this limiting curvature?

Secondly, we suggest that measurements of wave energy associated with specific ship designs be collected from instrumented buoys placed in Lac St Pierre during the summer operating season. This data would then be used to calibrate the aforementioned theoretical model.

Thirdly, we recommend that further field measurements of ice deflection, deformation, and water movement be conducted, with the goal of testing the above theoretical model under real conditions. This time, data collection at a much higher frequency (perhaps 10 Hz) and the bottom of the ice sheet would be instrumented to pick up tensile stresses.

Together, such a model would go far in instituting realistic guidelines for ship velocities in ice bounded navigation channels.

8. References

Beltaos, S. 2004. Wave-generated fractures in river ice covers. Cold Regions Science and Technology, v 40, n 3, December, 2004, p 179-191.

Beltaos, S., Rowsell R., 2001. Field study of pre-breaku p river waves. Proceedings (Available in CD Format), 11th Workshop on River Ice, Ottawa, pp. 4– 17.

Carter, D., Stander, E, and M. Hodgson, 1995. Ice Management in Lac St. Pierre. Transport Canada Publication No. TP 12439. 52. pp + appendices.

Cox, G. and J. Johnson. 1983. Ice Stress Measurements. U.S. Army CRREL report 83-23. 31 pp.

Daly, S.F., 1993. Wave propagation in ice-covered channels. ASCE Journal of Hydraulic Engineering 119 (8), 895– 910.

Daly, S.F., 1995. Fracture of river ice covers by river waves. Journal of Cold Regions Engineering, ASCE 9 (1), 41– 52.

Gold, L.W., 1971. Use of ice covers for transportation. Canadian Geotechnical Journal 8 (2), 170– 181.

Squire, V.A., Fox, C. 1992. On ice coupled waves. A comparison of data and theory. Proceedings of the International Conference on Ice Technology, Advances in Ice Technology, 1992, p 269, Aug 11-13 1992, Cambridge, MA, USA. Computational Mechanics Publ.

Steffler, R.M., Hicks, E.F., 1994. Discussion of bWave propagation on ice-covered channelsQ. ASCE Journal of Hydraulic Engineering 120 (12), 1478– 1480.

Xia, X., Shen, H.T., 2002. Nonlinear interaction of ice cover with shallow water waves in channels. Journal of Fluid Mechanics 467, 259– 268.

9. **Acknowledgements**

The field work presented in this paper was funded by and presented to the Transportation Development Centre and the Canadian Coast Guard, Quebec Region by Carter and Stander under the direction of Morse while at CCG. Some of the analytical work is a new recent contribution. The authors would like to especially thank Mr. Tom Pierce of TDC for his interest and support of this project. We appreciate the comments of the draft article by S. Dumont and L. Dupuis of CCG. Thanks also go to the officers of the "Bureau des glaces" and the Ice Patrol crew of the CCG for their participation in the project and time spent in helicopter surveillance. We also thank M. Hodgson for field support during the study.

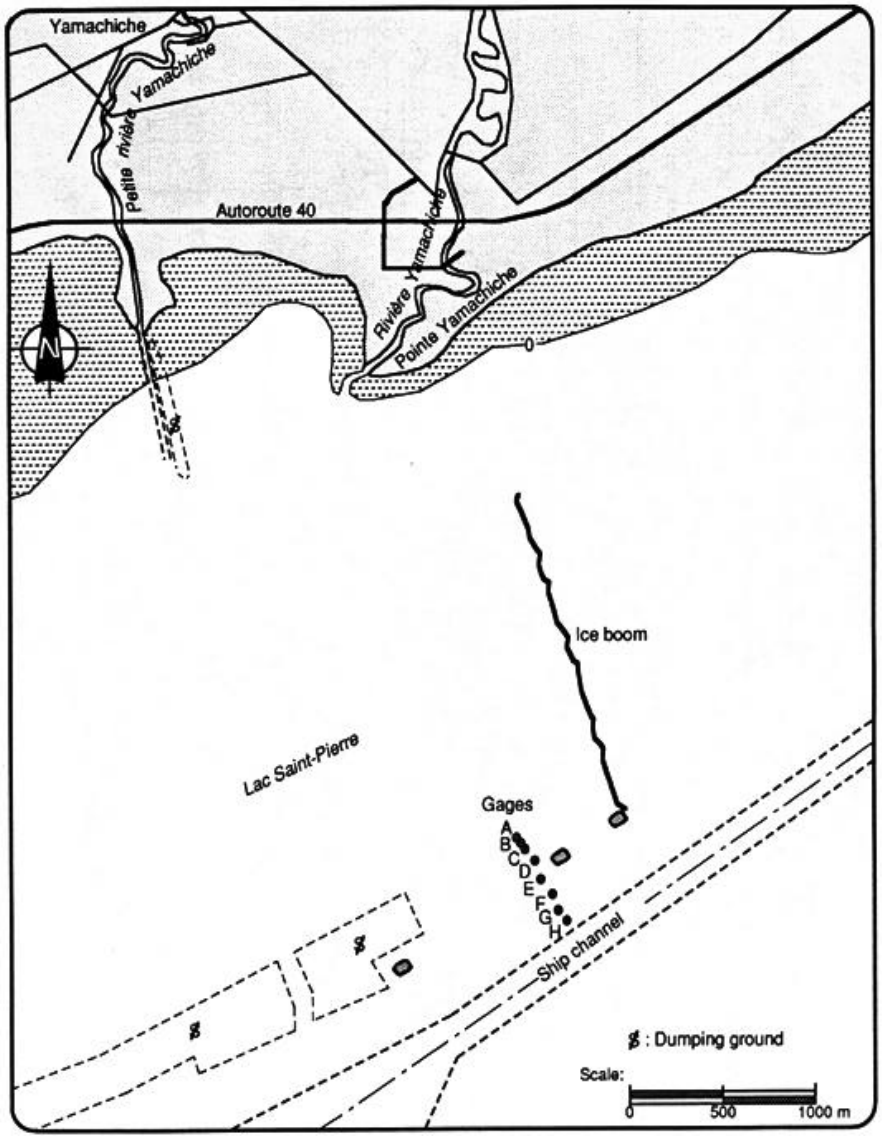

Figure 1: A general map of the study area

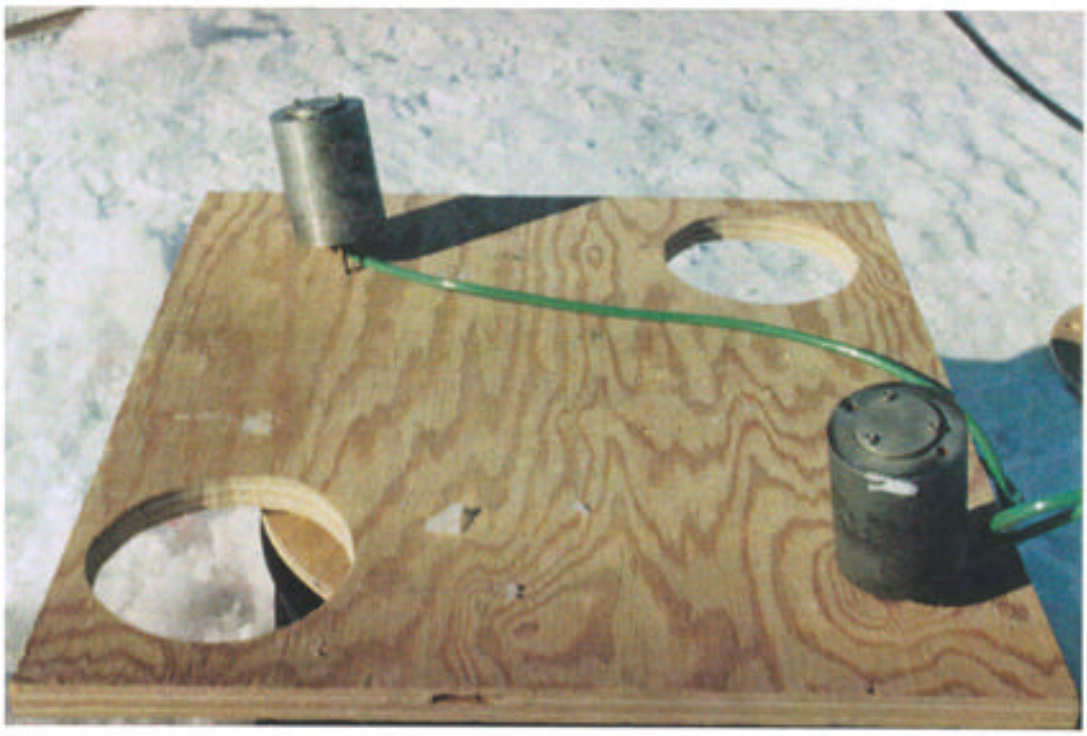

Figure 2: The Geokon stress gages ready for emplacement. Each gage contains two wires 90 degrees apart and the gages are orientated 45 degrees from one another.

Figure 3: the Endeco wire gage used to measure ice displacement. This gage was placed later in the season and employed a PVC tube to avoid the effect of pressure waves beneath the ice sheet.

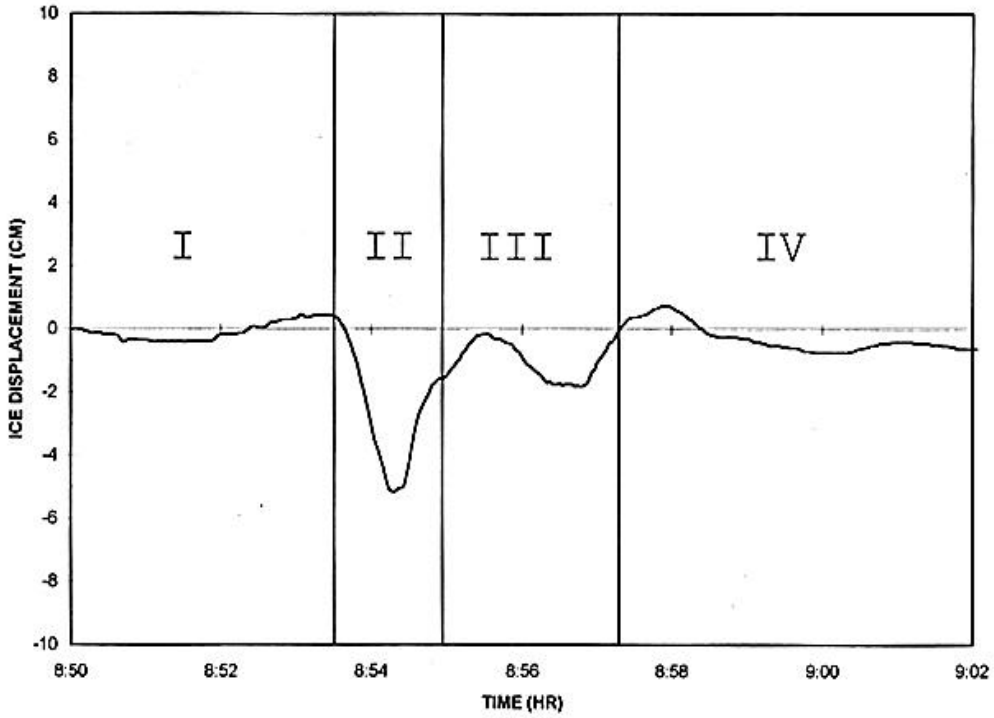

Figure 4: A typical displacement event: in this case the KAPITANAS Gudin, a bulk carrier which was encountered on February 18, 1995.

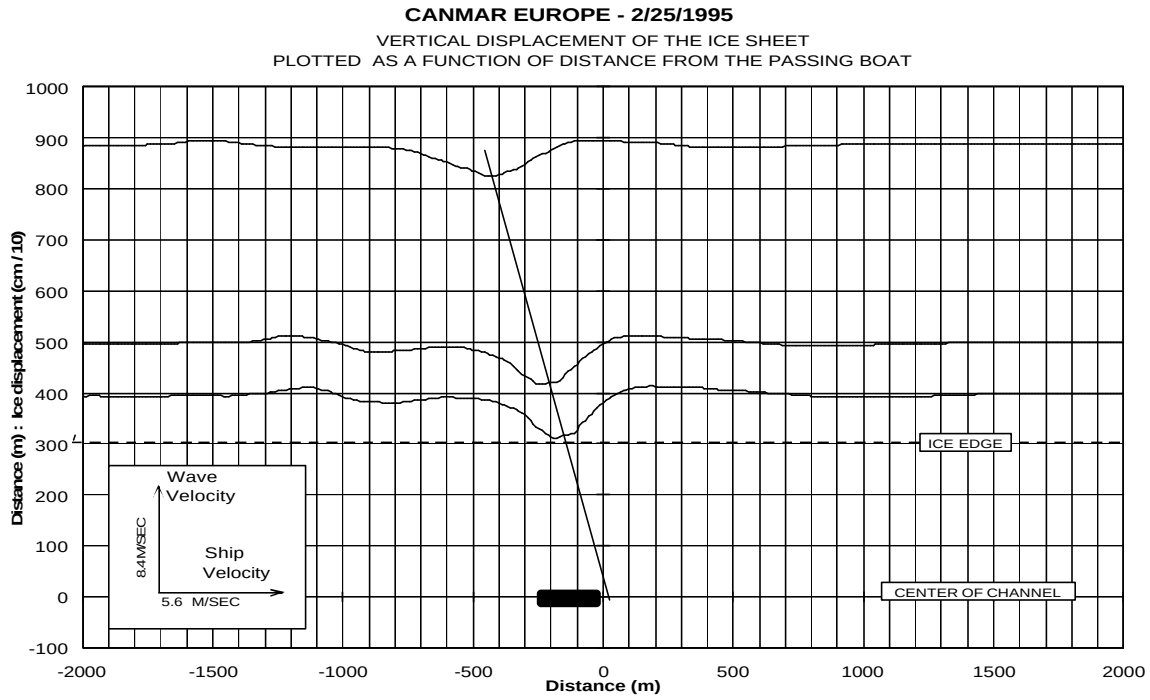

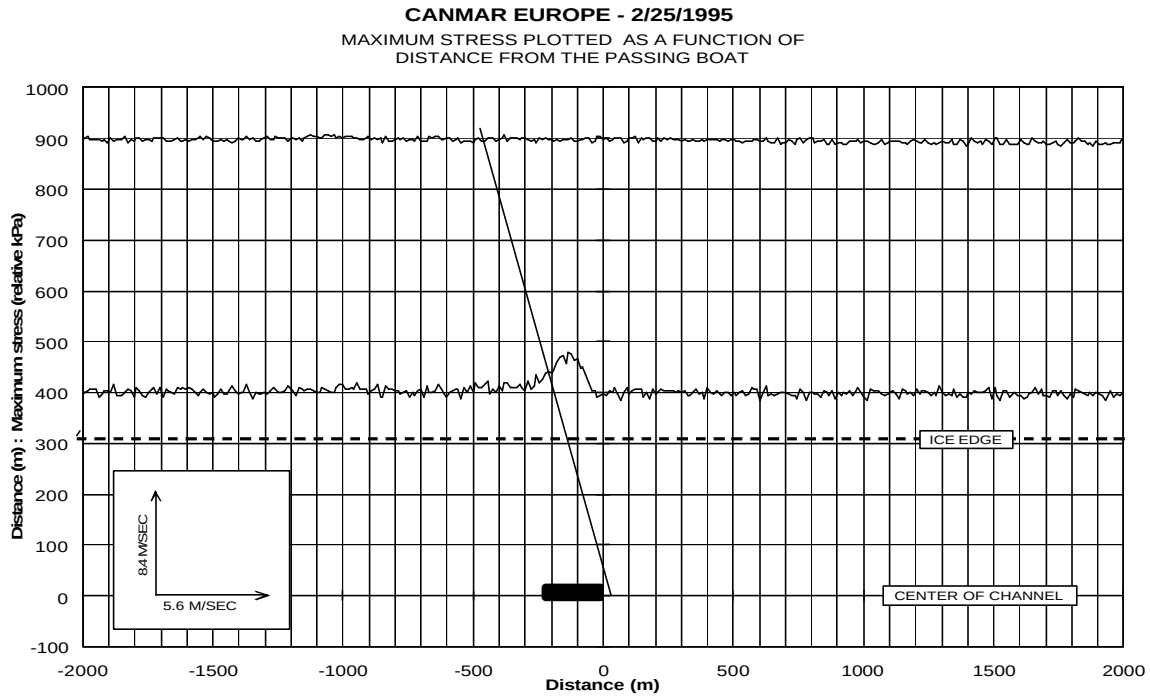

Figure 5a and 5b: A spatial map of ice displacement and maximum stress for the CANMAR Europe. The position of the Europe during the event is given by the black ellipse. The two arrows enclosed in the inset box give the measured ship velocity, and wave propagation velocity, respectively. Note that the measured wave front (the inclined black line) neatly crosses the bow of the passing Europe. Movement of the Europe was from left to right (downstream).

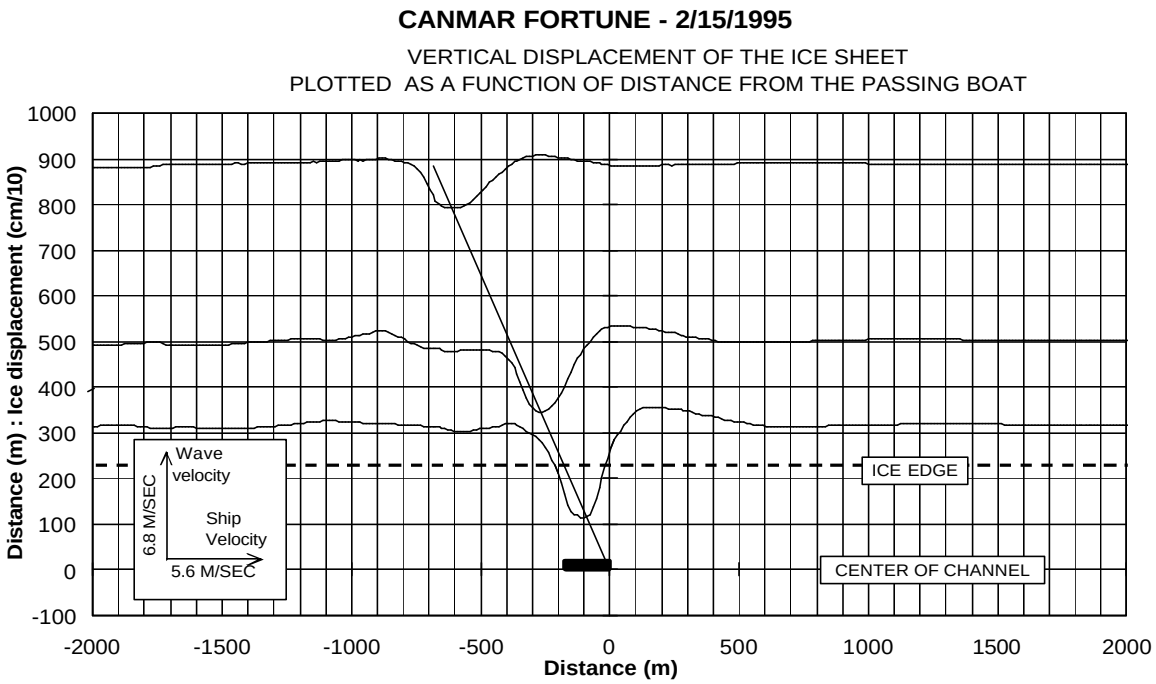

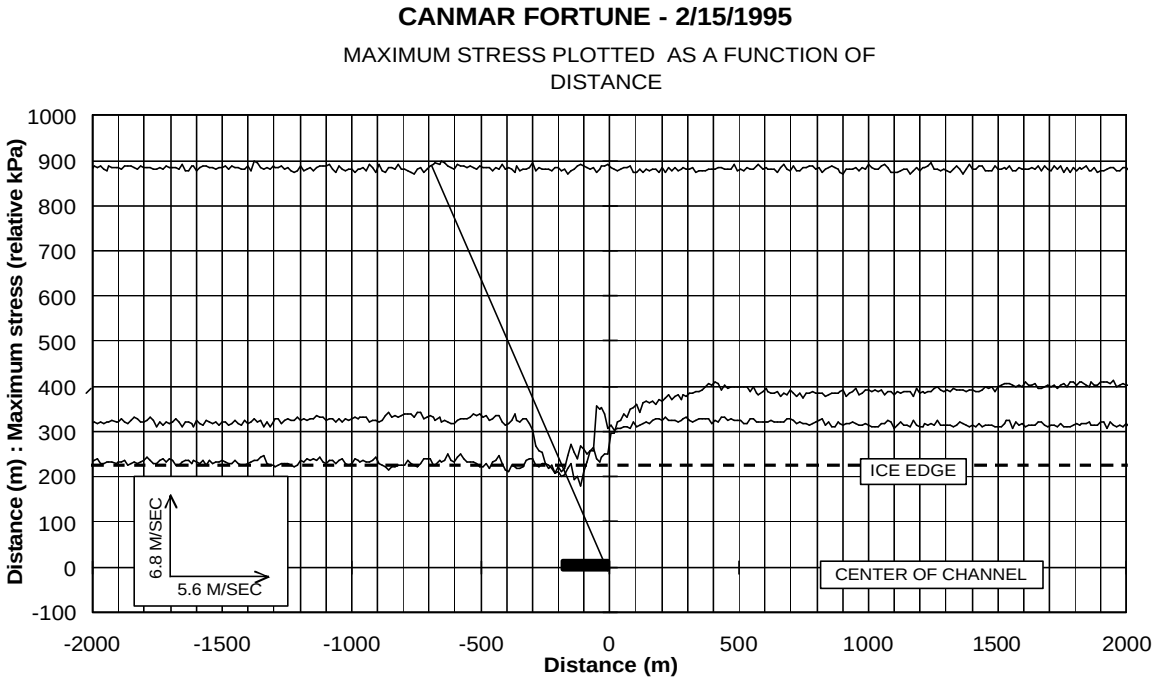

Figure 6a and 6b: A spatial map of ice displacement and maximum stress for the CANMAR Fortune. The position of the Fortune during the event is given by the black ellipse. The two arrows enclosed in the inset box give the measured ship velocity, and wave propagation velocity, respectively. Movement of the Fortune was from left to right (downstream).

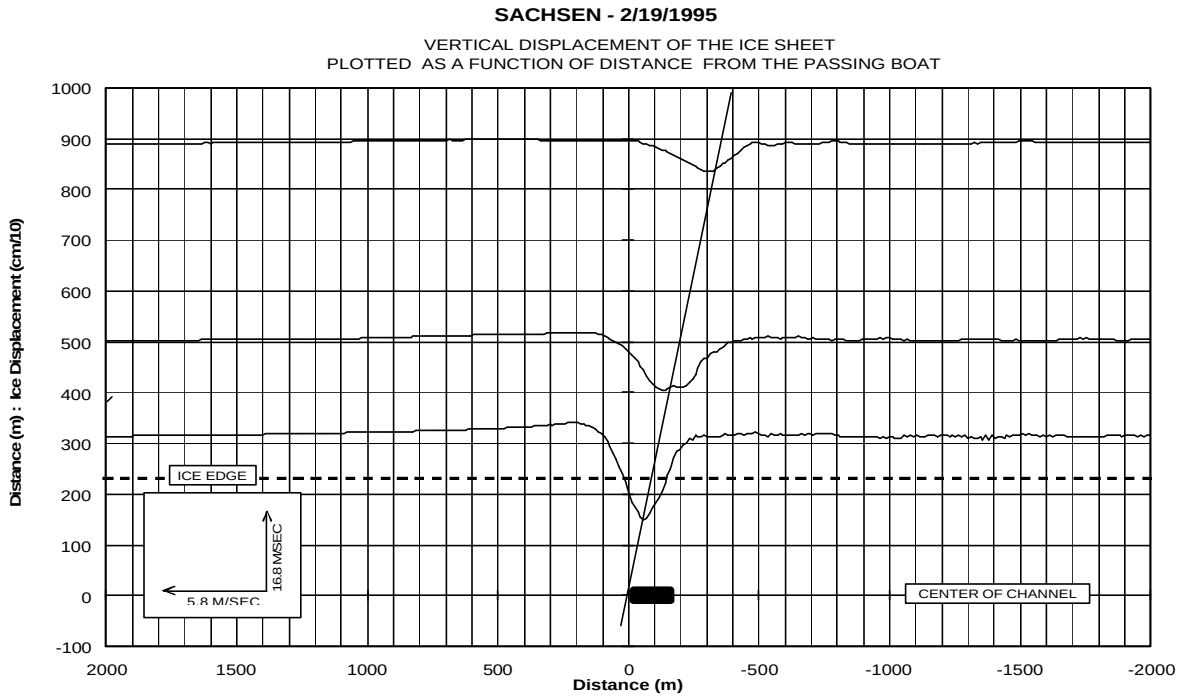

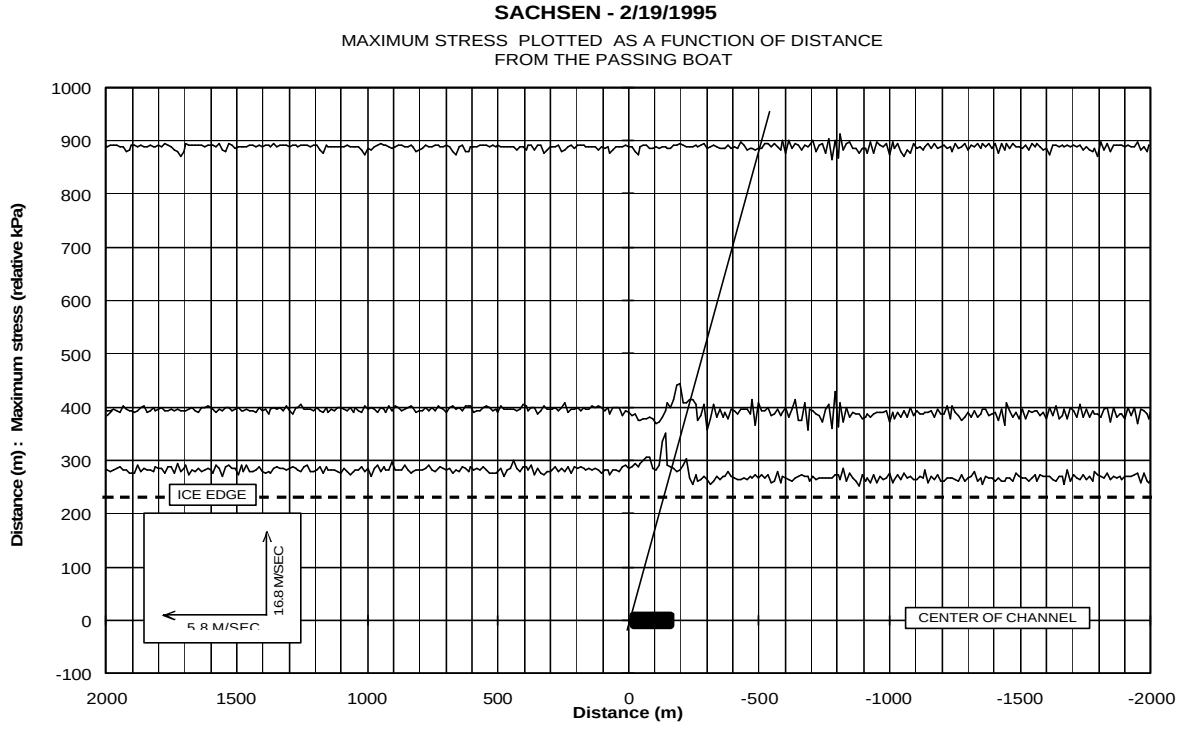

Figure 7a and 7b: A spatial map of ice displacement and maximum stress for the Sachen. The position of the Sachen during the event is given by the black ellipse. The two arrows enclosed in the inset box give the measured ship velocity, and wave propagation velocity, respectively. Movement of the Sachen was from right to left (upstream).

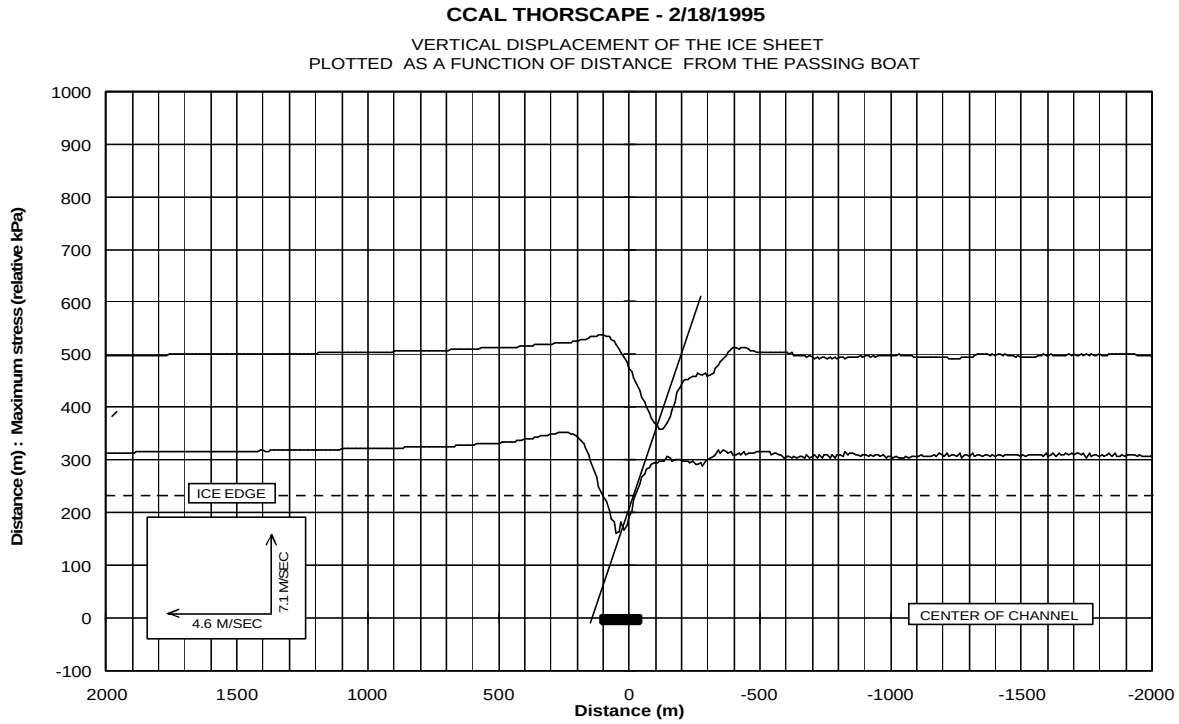

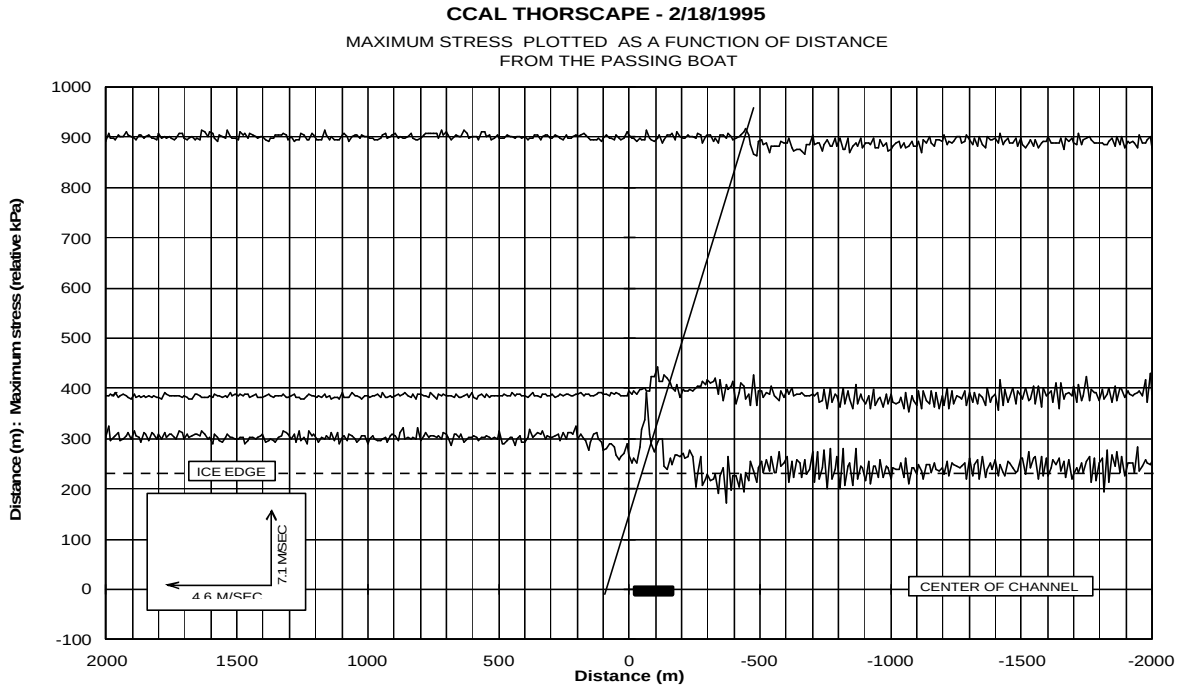

Figure 8a and 8b: A spatial map of ice displacement and maximum stress for the Thorscape. The position of the Thorscape during the event is given by the black ellipse. Movement of the Thorscape was from right to left (upstream).

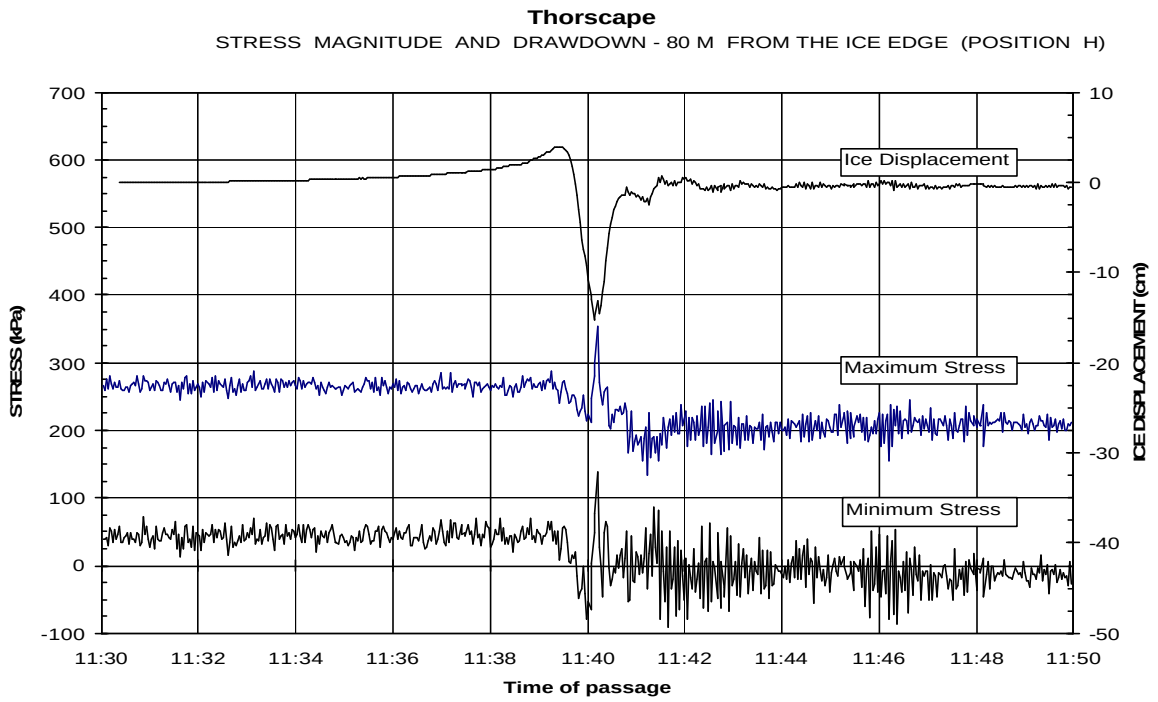

Figure 9: The relationship between drawdown and deformation in the ice sheet.
Break-up of the ice front probably occurred at the moment of flexure (as minimum stress dropped to zero).

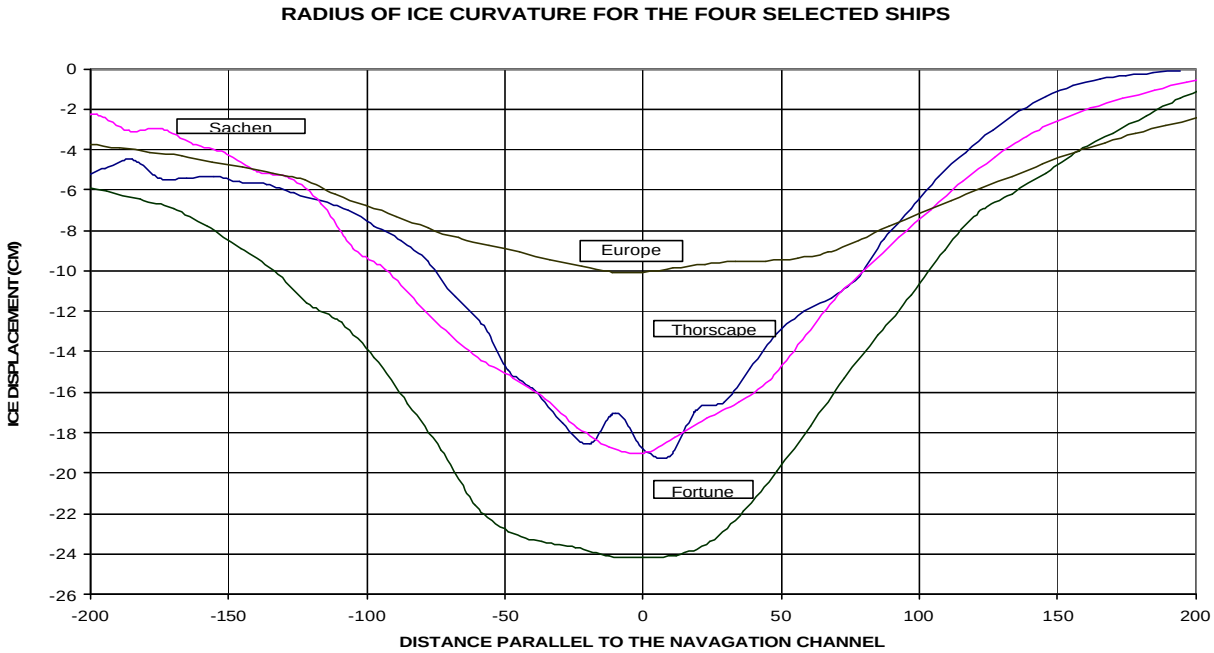

Figure 10: A comparison of the radius of ice curvature measured during the drawdown event of the Europe, Fortune, Sachen, and Thorscape. All measurements were collected within 80 meters of the ice edge.